

Experimental Verification of High-Resolution Wide-Swath Moving Target Indication

Stefan V. Baumgartner, German Aerospace Center (DLR), stefan.baumgartner@dlr.de, Germany
Gerhard Krieger, German Aerospace Center (DLR), gerhard.krieger@dlr.de, Germany

Abstract

In [1, 2] we have introduced a set of novel low pulse repetition frequency (PRF) algorithms, which allow for simultaneous high-resolution wide-swath (HRWS) SAR imaging and moving target indication (MTI) without the need of changing the system operation mode and the pulse repetition frequency (PRF). The core of these novel HRWS-MTI algorithms is the so called *Matched Reconstruction Filter Bank* (MRFB). By applying the MRFB, low PRF moving target signals can be reconstructed and refocused. Additionally, accurate estimates of the target motion parameters are obtained. In this paper the experimental verification of the MRFB principle is presented for the first time. For the verification real multi-channel airborne data acquired with DLR's F-SAR sensor over a maritime scenario are used.

1 Introduction

During the past years spaceborne surveillance of road, land and maritime traffic has evolved to an important research and security topic. However, in the spaceborne case classical MTI algorithms, which generally require high PRFs, cannot be used for monitoring wide areas or wide swaths. Due to timing issues high PRFs allow only for imaging relatively small swath widths and additionally may cause unacceptable large range ambiguities which destroy the image quality.

Novel low PRF MTI algorithms are needed for enabling a wide-swath and high-resolution MTI capability. Even if no clutter suppression is required, as this is for instance the case for ship monitoring at low sea states, most of the conventional HRWS reconstruction algorithms discussed so far in the literature are not able to reconstruct a moving target signal properly and to cancel its azimuth ambiguities, which are also called *Ghost Targets*.

In [1, 2] we have introduced some novel low PRF HRWS-MTI algorithms which allow for simultaneous HRWS SAR imaging and wide-swath MTI. With these algorithms moving target signals can be properly reconstructed and the velocities, moving directions and actual positions of the targets can be estimated accurately (remember that moving objects in SAR images generally appear smeared and displaced from their actual positions if no motion adapted processing is performed). The principles of the algorithms and Monte-Carlo simulation results are presented and discussed in detail in [1].

In the present paper the *Matched Reconstruction Filter Bank* (MRFB), which is the core of all novel low PRF HRWS-MTI algorithms introduced in [1, 2], is verified with real multi-channel X-band SAR data acquired with DLR's airborne sensor F-SAR [8]. The principle of the MRFB is shown in **Figure 1**. The HRWS reconstruction is adapted iteratively to the target's along- and across-track velocity components.

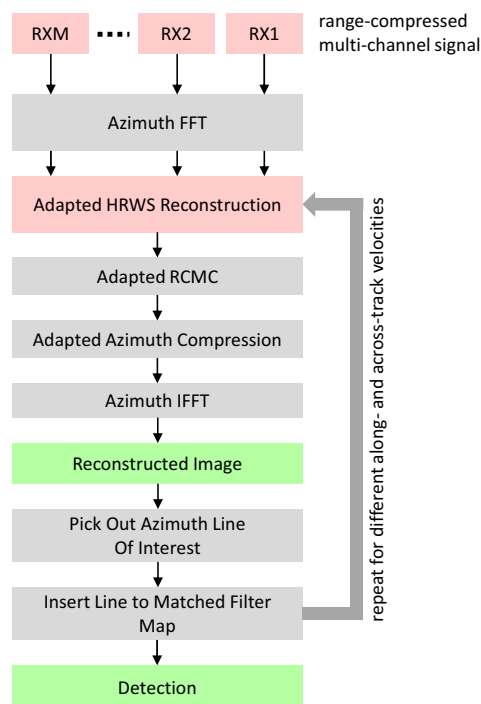


Figure 1: Principle of the MRFB introduced in [2].

2 F-SAR Sensor Configuration

For the experiments it is important that the PRF is chosen so that for a group of M adjacent receiving (RX) antennas the uniform sampling condition is fulfilled as good as possible. The required PRF is given as [1]

$$PRF_{HRWS} = \frac{2 v_p}{M \cdot L_{a,RX}} \quad (1)$$

where v_p is the platform velocity and $L_{a,RX}$ is the length of a single RX antenna.

In the F-SAR X-band configuration in total four RX antennas aligned in along-track direction are available [4]. For the proof of the MRFB concept it is sufficient to use only 3 of them. The antenna configuration used for the MRFB verification is sketched in **Figure 2**. Each RX antenna has a length of 20 cm.

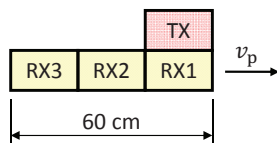


Figure 2: F-SAR X-band along-track antenna configuration.

For a typical F-SAR flight speed of $v_p = 85$ m/s the uniform sampling condition is fulfilled for $PRF_{HRWS} = 283.33$ Hz. For the experimental verification the data can principally be acquired with a n times higher PRF (n is an integer number). The low PRF situation (i.e., the uniform sampling condition) is then obtained by subsampling, i.e., by just skipping temporal azimuth samples. From the investigation point of view this has the advantage that the high PRF images can be used as a reference for performance comparison purposes.

3 Experimental Results

The multi-channel F-SAR data used for verifying the MRFB algorithm were acquired during an ocean surface measurement campaign in Northern Germany in 2009. A high PRF of 2016.13 Hz was used during the experiments. For verification a data take containing land mass as well as a number of moving ships was chosen (cf. **Figure 3**). The presence of the land mass has the advantage, that it can be used for calibration purposes and for checking if the conventional HRWS reconstruction for stationary targets works correctly.

The system parameters are listed in **Table 1**.

Parameter	Value
Center frequency	9.6 GHz
Wavelength λ	0.0312 m
Range r_{10} at center of Detail 1,2 and 3	4290 m
Range bandwidth	300 MHz
Platform velocity v_p	85.81 m/s
Average squint angle	$\approx 9.04^\circ$
Original PRF	2016.13 Hz
Desired PRF_{HRWS} computed with (1)	286.05 Hz
Actual PRF_{HRWS} after subsampling	288.02 Hz

Table 1: System parameters during the experiment.

It has to be noted that the comparatively large squint angle of 9.04° causes an average Doppler centroid of approximately 900 Hz as can be seen in **Figure 4**, where the high PRF Doppler spectra of the image patch labeled with Detail 2 in **Figure 3** is plotted. The Doppler centroid

has to be considered for obtaining a successful HRWS reconstruction.

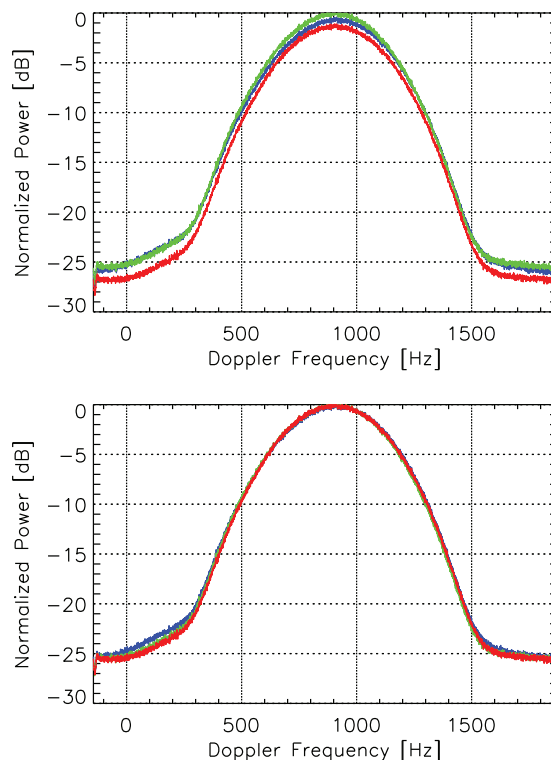


Figure 4: High PRF Doppler spectra of the channels RX1 (blue), RX2 (green) and RX3 (red) before channel balancing (top) and afterwards (bottom).

3.1 Data Preparation

Data preparation involves calibration, channel balancing and subsampling of the high PRF data to the much lower PRF_{HRWS} .

For estimating the channel imbalances the high PRF data patch labeled with Detail 2 in **Figure 3** was used. Only the average amplitude of each channel and the along-track interferometric (ATI) phases after coregistration of RX2 and RX3 with the reference channel RX1 were estimated. The estimated amplitudes and ATI phases can afterwards be applied on arbitrary range-compressed data patches, e.g., on the patches Detail 1 and Detail 2, for balancing RX2 and RX3 with RX1 (cf. **Figure 4** bottom). Note that the coregistration is only necessary for estimating the ATI phases needed for calibration purposes. For performing any HRWS reconstruction, the data must not be coregistered. A comparison of different calibration techniques is presented in [6].

After calibration the data were subsampled for obtaining the low PRF data. Subsampling was simply done by keeping only every 7th azimuth sample of the original range-compressed data. The PRF after subsampling differs only by 2 Hz from the PRF needed for fulfilling perfectly the uniform sampling condition (cf. **Table 1**).

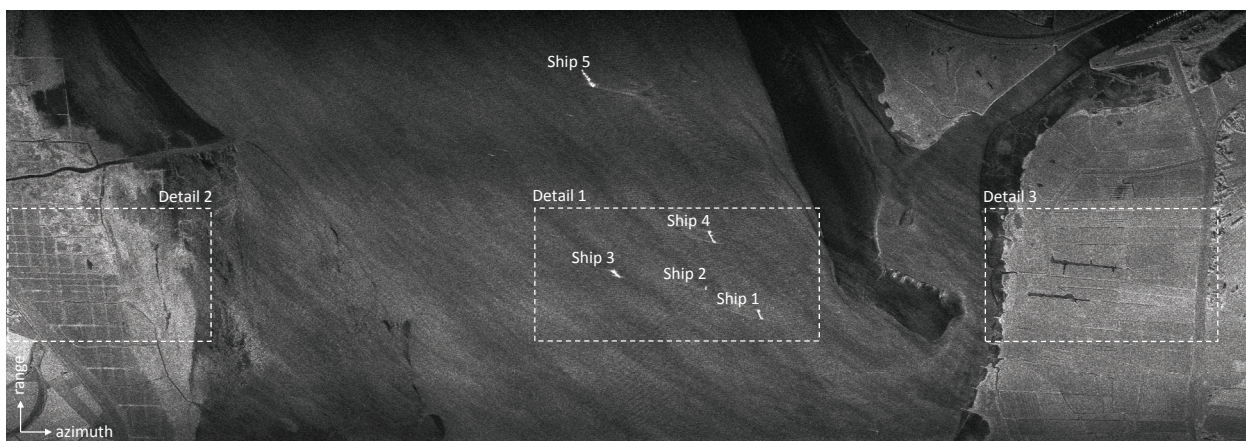


Figure 3: High PRF reference SAR image of the mouth of the river Elbe in the North Sea, Germany. The data contains moving ships (Detail 1) and land masses (Detail 2 and Detail 3). The data were acquired with the F-SAR sensor under high squint angle conditions (datatake ID 09tdxsim0104).

3.2 Conventional HRWS Reconstruction

For a conventional HRWS reconstruction of the stationary world the *Maximum Signal Method* discussed in [7] was applied after adapting the baseline delay matrix properly to the comparatively large squint angle of the data. The obtained image results after performing the reconstruction are shown in **Figure 6** at the bottom. The patches labeled with Detail 2 and Detail 3 are properly reconstructed and focused as expected, since they contain only the stationary world without moving targets. The reconstructed Doppler spectrum of Detail 2 is depicted in **Figure 5**.

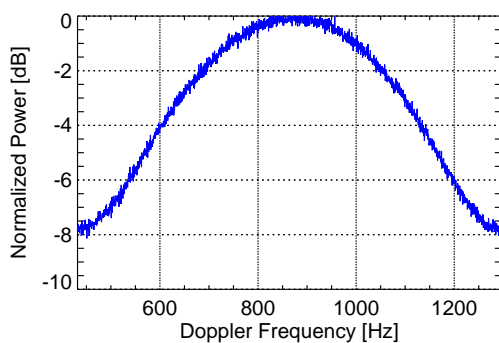


Figure 5: Reconstructed Doppler spectra of Detail 2.

In Detail 1, where 4 moving ships are present, a number of azimuth ambiguities can clearly be recognized. These ambiguities or *Ghost Targets* are caused due to a mismatch of the conventional HRWS reconstruction filter, as explained in detail in [1]. The ambiguities appear also displaced in range due to a mismatched range cell migration correction and due to the comparatively high squint angle of 9.04° .

For azimuth focusing of the data contained in Detail 1, no Doppler bandpass filtering was applied so that the entire energy of the moving ships is preserved. The 3-dB Doppler bandwidth of the signals is approximately 450

Hz (cf. **Figure 5**), the corresponding illumination time is in the order of 4 s.

In the high PRF reference images (**Figure 6** top) the azimuth displacements of Ship 1 and Ship 4 clearly can be recognized. Due to the long integration time, the along-track velocity components of the ships as well as potential roll and pitch motion may cause significant quadratic and higher order phase errors which result in image blurring. Blurring effects are not so pronounced in the reconstructed HRWS images (**Figure 6** bottom), since the integration time of each *Ghost Target* is smaller owing to the smaller Doppler bandwidth interval determined by PRF_{HRWS} . The *Ghost Targets* belonging to Ship 2 and 3 are overlapping and, hence, difficult to assign to the actual target.

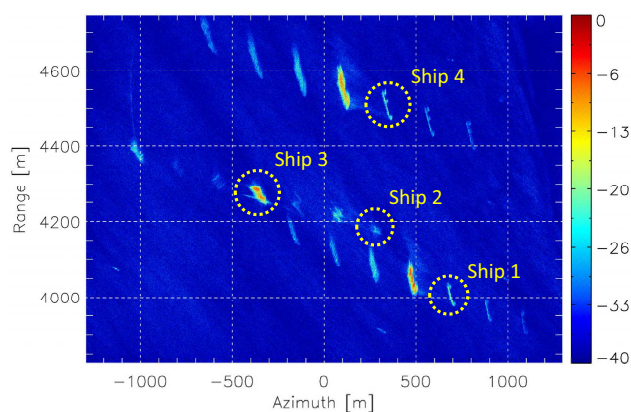


Figure 7: Conventionally HRWS reconstructed and SAR focused image of Detail 1. The power is normalized to the brightest image pixel, the values of the color bar are in dB. The yellow circles mark the ship positions obtained from the corresponding high PRF reference image (cf. **Figure 6** top).

For a better visual interpretation of the power and ambiguity ratios the conventionally HRWS reconstructed and SAR focused Detail 1 is again depicted in **Figure 7** with a different color table and in logarithmic scale. The power

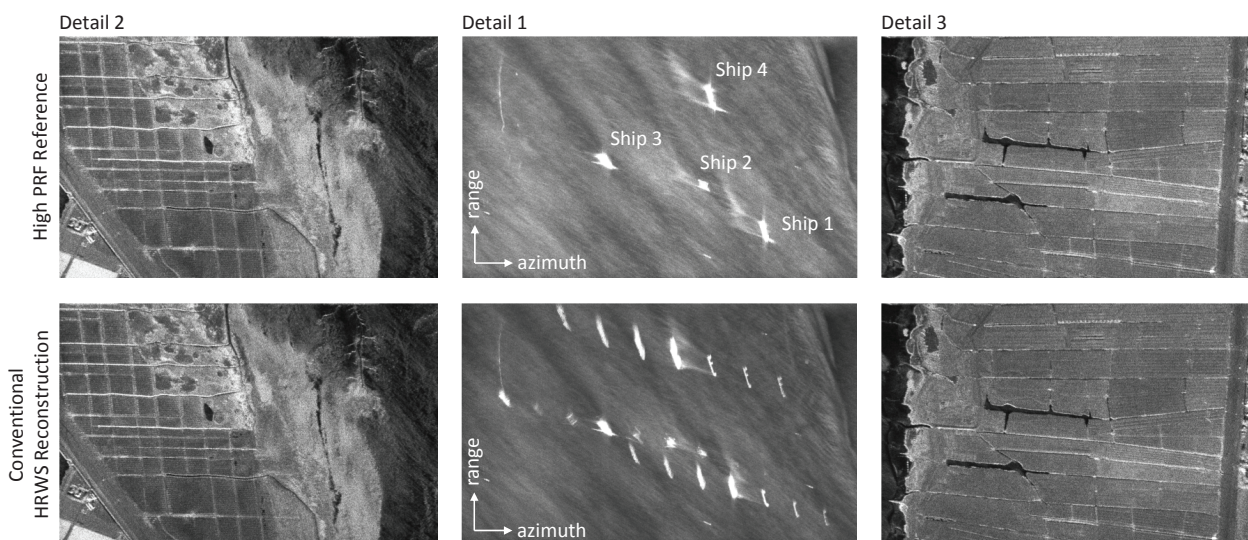


Figure 6: High PRF reference image patches (top) of the details marked in **Figure 3** and corresponding image results after conventional HRWS reconstruction and SAR focusing not adapted to moving targets (bottom). The large number of *Ghost Targets* can clearly be recognized in the Detail 1 patch at the bottom.

is normalized to the brightest image pixel.

By comparing the brightest *Ghost Targets* in **Figure 7** with the ship positions in the corresponding high PRF image patch (cf. **Figure 6** top), a position difference can be recognized. For an easier comparison the ship positions obtained from the corresponding high PRF reference image are marked with a yellow circle in **Figure 7**. After performing successfully a motion adapted HRWS reconstruction with the MRFB, the "real" reconstructed ships would appear at the same "displaced" positions as in the high PRF reference image. This behavior is a prerequisite for being able to compute the actual ship positions with high accuracy (remember that moving ships generally appear displaced in conventional SAR images as well as in reconstructed low PRF SAR images).

3.3 Motion-Adapted HRWS Reconstruction

For reconstructing the signals of the moving ships the MRFB is applied. The MRFB is an iterative application of motion adapted HRWS reconstruction beamformers as depicted in **Figure 1** and explained in detail in [1]. After each iteration a motion adapted HRWS image is obtained. The best across-track velocity match maximizes the amplitude of the output image and, even more important, attenuates the target's azimuth ambiguities or *Ghost Targets* significantly. Some image examples for Ship 1 are shown in **Figure 8**. In this example for an across-track velocity of $v_{y0} = -6$ m/s the *Ghost Targets* are strongly attenuated and the reconstructed Ship 1 appears at the same position as in the high PRF reference image.

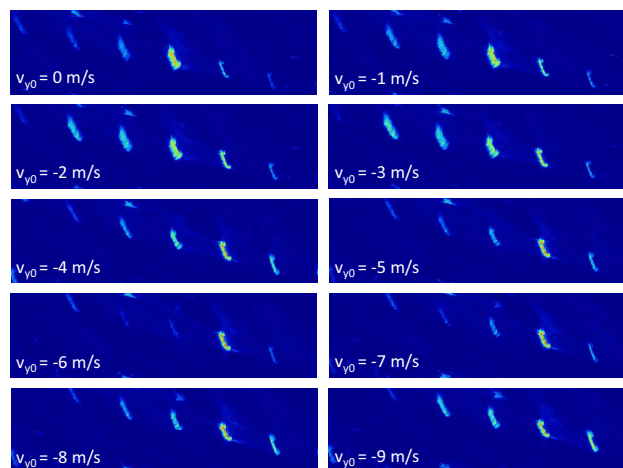


Figure 8: Motion adapted reconstructed SAR images of Ship 1 obtained after application of the MRFB. It can be seen that for an across-track velocity of $v_{y0} = -6$ m/s all *Ghost Targets* are significantly attenuated. The output amplitudes are normalized to the maximum amplitude output provided by the MRFB after all conducted iterations. The same logarithmic scale and color bar as in **Figure 7** is used.

A more detailed comparison between the images corresponding to 0.0 m/s and to -5.9 m/s (= best match) across-track velocity is shown in **Figure 9**. The amplitudes of the *Ghost Targets* in the conventionally HRWS reconstructed SAR image (top) are in the order of -10 to -35 dB w.r.t. the maximum amplitude obtained from the MRFB. In the motion adapted image (bottom) no *Ghost Target* is larger than -30 dB. Additionally, the "real" ship appears, as desired, at the same position as in the high PRF reference image (cf. **Figure 6** top). Note that the ambiguity levels have only roughly been estimated in steps of 5 dB. Since the target as well as the ambiguities occupy more than one resolution cell, a more precise evaluation would

require to consider the amplitude distributions.

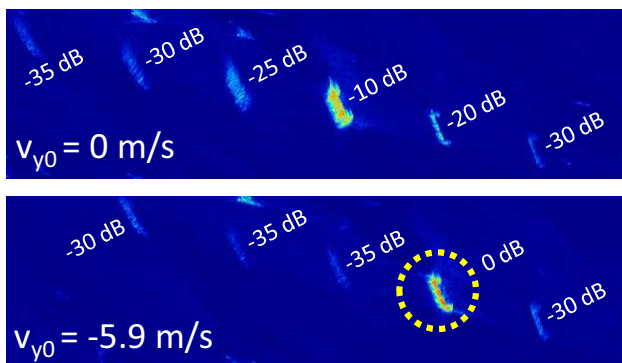


Figure 9: Results obtained for Ship 1 for an across-track velocity of 0.0 m/s (top) and -5.9 m/s (bottom). The velocity of -5.9 m/s leads to the best reconstruction result for Ship 1. The position of the yellow circle corresponds to the position of Ship 1 in the high PRF reference image.

The same investigations as for Ship 1 have been carried out for Ship 4. The results are depicted in **Figure 10**. Again, after correct motion adapted reconstruction the ship appears at the same position as in the high PRF reference image and the *Ghost Targets* are significantly attenuated.

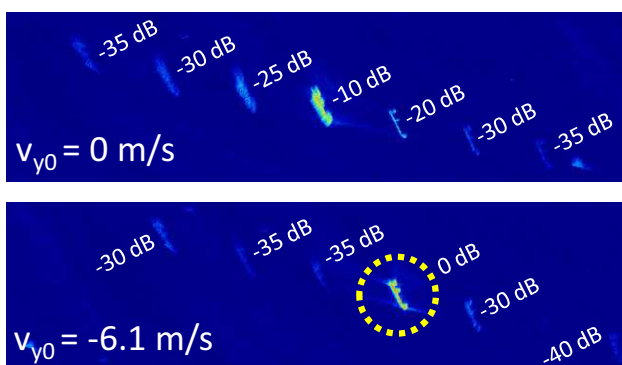


Figure 10: Results obtained for Ship 4 for an across-track velocity of 0.0 m/s (top) and -6.1 m/s (bottom). The velocity of -6.1 m/s leads to the best reconstruction result for Ship 4. The position of the yellow circle corresponds to the position of Ship 4 in the high PRF reference image.

The across-track velocity estimates obtained with the MRFB for Ship 2 and 3 are -5.25 and -0.5 m/s. Due to the lack of space the corresponding image results are not presented in the paper.

All results presented so far are for an assumed along-track velocity component of $v_{x0} = 0.0$ m/s. If in the MRFB additionally the along-track velocity component is iteratively adapted (which needs more computation power since more iterations are required), the second order phase errors of a moving target can be compensated so that it appears refocused in azimuth. The consideration of the correct along-track velocity further increases the signal amplitude and the signal-to-clutter plus noise ratio (SCNR) as well as the signal to ambiguity ratio. An example for Ship 1 is depicted in **Figure 11**. The best match

is obtained for an along-track velocity of $v_{x0} = -1.0$ m/s and an across-track velocity of $v_{y0} = -5.9$ m/s.

With the estimated across-track velocity the actual target position can be computed unambiguously [3]. Together with the estimated along-track velocity the motion direction can be determined. However, similar as for conventional MTI algorithms, the along-track velocity estimation is biased by across-track accelerations [5].

By applying the MRFB in a dense multi-target scenario it is generally not possible to obtain an image where all moving targets or ships appear correctly reconstructed and focused at the same time. Each individual target needs a different motion adapted reconstruction filter, especially if all the targets in the scene move with different across-track velocities.

4 Conclusions

It has been shown that a conventional HRWS algorithm is not capable for reconstructing low PRF moving target signals correctly. It introduces a number of *Ghost Targets* as depicted in **Figure 7** and in **Figure 6** at the bottom. A discrimination between the ghosts and the "real" targets might be challenging. Furthermore, the actual target positions cannot be determined as long as it is not clear which are the *Ghost Targets* and which are the "real" targets.

In the paper it was verified by using real multi-channel data, that the application of the MRFB [1], where a motion adaptive reconstruction is performed iteratively, can solve these problems. The MRFB not only delivers the reconstructed moving target signals, but also provides estimates of the target across- and along-track velocity.

For future spaceborne HRWS SAR systems with maritime applications in mind, the potential occurrence of *Ghost Targets* has to be considered for the processor design.

References

- [1] Stefan V. Baumgartner and Gerhard Krieger. Simultaneous High-Resolution Wide-Swath SAR Imaging and Ground Moving Target Indication: Processing Approaches and System Concepts. *IEEE Journal of Selected Topics in Applied Earth Observations and Remote Sensing*, 8(11):5015–5029, November 2015.
- [2] Stefan V. Baumgartner, Christoph Schaefer, and Gerhard Krieger. Simultaneous Low PRF GMTI and HRWS SAR Imaging without Changing the System Operation Mode. In *10th European Conference on Synthetic Aperture Radar (EUSAR)*, pages 981–984, Berlin, Germany, June 2014.
- [3] Stefan Valentin Baumgartner and Gerhard Krieger. Multi-Channel SAR for Ground Moving Target Indication. In Rama Chellappa and Sergios Theodoridis, editors, *Academic Press Library in Signal Processing: Communications and Radar Signal Processing*, volume 2, chapter 18, pages 911–986. Academic

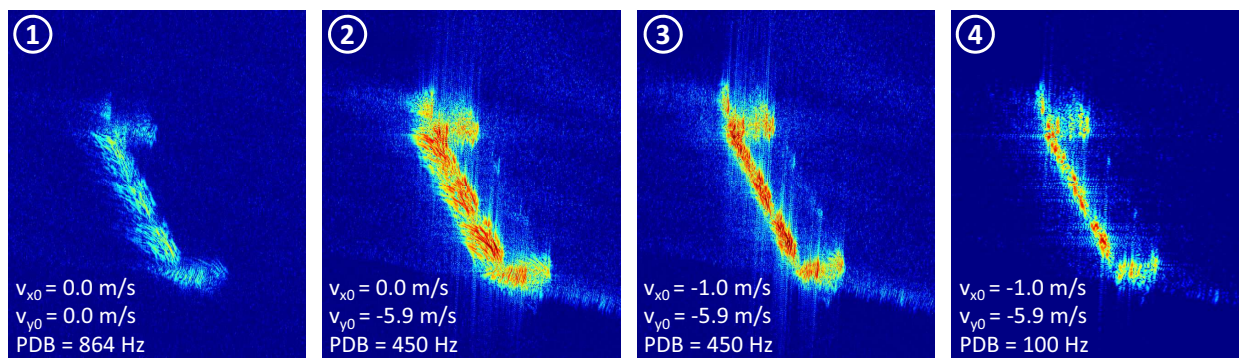


Figure 11: Images of Ship 1 after motion adapted HRWS reconstruction with different along- and across-track velocity assumptions. The best focusing result is obtained for $v_{x0} = -1.0$ m/s and $v_{y0} = -5.9$ m/s (cf. patch labeled with 3 and 4). For patch 2 and 3 a processed Doppler bandwidth (PDB) of 450 Hz (= 3dB bandwidth of the reconstructed Doppler spectrum) was used. The bandpass filter was centered around the Doppler bin corresponding to the Doppler shift caused by the across-track velocity v_{y0} . In patch 4 the processed Doppler bandwidth was reduced to 100 Hz. As a consequence the ship appears sharper, since the higher order phase errors due to the shorter observation time play a less important role. Patch 1 is just shown as a reference. It represents the imaging result obtained after applying a conventional HRWS reconstruction for a non-moving target. The maximum amplitude is more than 20 dB weaker (see also **Figure 9**).

Press (ELSEVIER), ISBN 978-0-12-396500-4, UK and USA, 1 edition, 2014.

- [4] S.V. Baumgartner, M. Gabele, N. Gebert, R. Scheiber, G. Krieger, K.-H. Bethke, and A. Moreira. Digital Beamforming and Traffic Monitoring Using the new F-SAR System of DLR. In *International Radar Symposium (IRS)*, Cologne, Germany, September 2007.
- [5] S.V. Baumgartner and G. Krieger. Acceleration-independent along-track velocity estimation of moving targets. *IET Radar Sonar Navigation*, 4(3):474–487, 2010.
- [6] Andrés Bertetich. Investigation of Multi-Channel SAR Calibration Methods for Real-Time Traffic Monitoring. Master’s thesis, Department of Information Engineering and Computer Science, University of Trento, October 2010.
- [7] Delphine Cerutti-Maori, Ishuwa Sikaneta, Jens Klare, and Christoph H. Gierull. MIMO SAR Processing for Multichannel High-Resolution Wide-Swath Radars. *IEEE Transactions on Geoscience and Remote Sensing*, 52(8):5034–5055, August 2014.
- [8] Andreas Reigber, Rolf Scheiber, Marc Jäger, Pau Prats, Irena Hajnsek, Thomas Jagdhuber, Kostas Papathanassiou, M. Naninni, E. Aguilera, Stefan Baumgartner, Ralf Horn, Anton Nottensteiner, and Alberto Moreira. Very-High-Resolution Airborne Synthetic Aperture Radar Imaging: Signal Processing and Applications. *Proceedings of the IEEE*, 101(3):759–783, March 2013.